Universal quantum computation in a neutral-atom decoherence-free subspace

E. Brion,* L. H. Pedersen,† and K. Mølmer
Lundbeck Foundation Theoretical Center for Quantum System Research, Department of Physics and Astronomy, University of Aarhus, Ny Munkegade, Building 1520, DK-8000 Århus C, Denmark

S. Chutia and M. Saffman
Department of Physics, University of Wisconsin, 1150 University Avenue, Madison, Wisconsin 53706, USA
(Received 24 November 2006; published 21 March 2007)

In this paper, we propose a way to achieve protected universal computation in a neutral-atom quantum computer subject to collective dephasing. Our proposal relies on the existence of a decoherence-free subspace (DFS), resulting from symmetry properties of the errors. After briefly describing the physical system and the error model considered, we show how to encode information into the DFS and build a complete set of safe universal gates. Finally, we provide numerical simulations for the fidelity of the different gates in the presence of time-dependent phase errors and discuss their performance and practical feasibility.

DOI: 10.1103/PhysRevA.75.032328 PACS number(s): 03.67.Lx, 32.80.Qk, 32.80.Rm

I. INTRODUCTION

Within the last few years, quantum information has become one of the most promising and active fields in physics. In the commonly used model, a quantum computer consists of two-level systems, the qubits, in which information is stored in a binary fashion. Calculations on this information are achieved through the application of particular evolutions of the system, called quantum gates [1]. Thanks to quantum parallelism [2], which merely follows from the linearity of quantum mechanics, quantum computers are expected to be much more efficient than their classical analogs, in particular for simulating the behavior of quantum systems [3] and for solving some "difficult" problems, such as factoring [4]. Unfortunately, none of the various experimental proposals, comprising NMR [5], cavity quantum electrodynamics [6], and trapped-ion [7] implementations, has succeeded in satisfying all the requirements one has to check in order to design a valuable quantum computer, known as DiVincenzo's criteria [8]. In particular, decoherence, which arises from the interaction of the system with its environment, remains a major obstacle to the feasibility of quantum computing.

Quantum gates may be implemented with neutral atoms using either short-range collisions or long-range dipole-dipole interactions. The proposal of Jaksch *et al.* [9] suggested using the strong dipole-dipole interactions of highly excited Rydberg atoms for fast quantum gates. In a recent paper [10], Saffman and Walker provided a detailed study of the Rydberg scheme using optically trapped ^{87}Rb atoms. In particular, it was shown that the errors due to the trap setup itself can be made quite small by a proper choice of physical parameters, allowing for fast and reliable single- and two-qubit gates.

In this paper, we elaborate on this proposal by considering the effect of collective random dephasing errors, which, for instance, stem from the uncontrolled action of exterior fields. In Sec. II, we briefly present the physical implementation proposed in [10], as well as the error model we choose to address and we show how to protect information through encoding into a decoherence-free subspace (DFS), the existence of which merely follows from the symmetry properties of the errors. In Sec. III, we build a complete set of universal protected gates, which allows us to perform any computation without leaving the DFS. In Sec. IV, we provide numerical simulations for the fidelity of the different gates in the presence of time-dependent phase errors. The practical feasibility of these gates is then discussed; in particular, the limitation arising from spontaneous emission is addressed. Finally, in Sec. V, we give our conclusions and the perspectives of our work.

II. A NEUTRAL-ATOM QUANTUM COMPUTER

The quantum-computing proposal we shall consider throughout this paper has been put forward recently in [10]. The physical qubit consists of a ^{87}Rb atom restricted to the hyperfine states

$$|0\rangle \equiv |5S_{1/2}, F=1, m_F=0\rangle,$$

$$|1\rangle \equiv |5S_{1/2}, F=2, m_F=0\rangle,$$

which form the logical basis (see Fig. 1). After precooling in a magneto-optical trap, the different qubits which constitute the computer are captured in an eggbox-style potential created by a far-off-resonance trap (for a detailed presentation

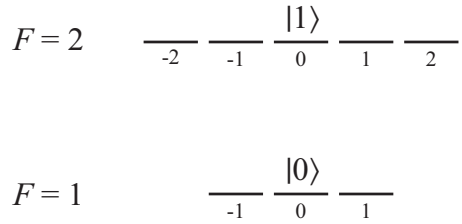

FIG. 1. Qubit basis states.

*Electronic address: ebrion@phys.au.dk
†Electronic address: lhp@phys.au.dk

of the technical aspects of the physical apparatus, see [10]).

In this setting, the single-qubit rotations are implemented through Raman-like transitions between $|0\rangle$ and $|1\rangle$ via an off-resonance excited state, whereas the two-qubit phase gate is performed according to Jaksch *et al.*'s proposal [9] which relies on the large dipole-dipole interaction between Rydberg atoms. Combining single-qubit rotations and two-qubit phase gates leads to the standard set of universal quantum gates, comprising the single-qubit Hadamard (H) and $\pi/8$(T) gates, as well as the two-qubit controlled-NOT (CNOT) gate:

$$H \equiv \frac{1}{\sqrt{2}}\begin{bmatrix} 1 & 1 \\ 1 & -1 \end{bmatrix}, \quad T \equiv \begin{bmatrix} 1 & 0 \\ 0 & e^{i\pi/4} \end{bmatrix},$$

$$\text{CNOT} \equiv \begin{bmatrix} 1 & 0 & 0 & 0 \\ 0 & 1 & 0 & 0 \\ 0 & 0 & 0 & 1 \\ 0 & 0 & 1 & 0 \end{bmatrix}.$$

Analyzing the error sources due to the trap setup (background gas collisions, scattering of the trapping light, heating due to laser noise, etc.), the authors of [10] show that, given a proper choice of the physical parameters, single- and two-qubit gates can be performed at megahertz rates with decoherence probability and fidelity errors at the level of 10^{-3}.

In this paper, we shall consider the effect of random phase errors which affect different qubits according to the same (*a priori* time-dependent) error Hamiltonian

$$\hat{E}(t) = \hbar \begin{bmatrix} \epsilon_0(t) & 0 \\ 0 & \epsilon_1(t) \end{bmatrix}.$$

Typically, this kind of error model stands for the action of parasitic external fields which induce uncontrolled and unwanted energy shifts. If no protection scheme is used, the unknown differential phase shift induced by $\hat{E}(t)$ on the qubit states rapidly leads to a complete loss of coherence.

III. PROTECTION AGAINST THE ERRORS THROUGH ENCODING INTO A DFS

A. Secure storage of the information in a DFS

To protect information from quantum errors, one can resort to active schemes such as quantum codes [1], the most famous example being the stabilizer codes [11]. It is also possible to take advantage of the symmetry properties of the interaction between the system and its environment in order to passively protect information from the effects of decoherence; this is the basic principle of the decoherence-free subspace strategy [12], which consists in encoding information into subspaces immune to errors. The explicit construction of a DFS has already been achieved for certain collective [13], noncollective [14], and arbitrary [15] error processes and even experimentally implemented in quantum optics [16], trapped-ion [17], neutral-atom [18], and NMR [19] setups. Moreover, universal computation within these DFS's has been shown to be possible from a theoretical point of view [20]. Here, we shall deal with the practical implementation

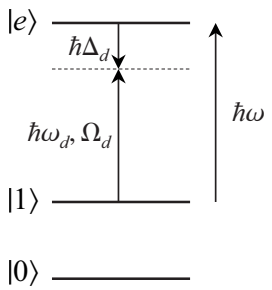

FIG. 2. Level scheme for the dephasing gate.

of such a DFS in the neutral-atom system described in [10].

In the case of collective dephasing, a DFS can be straightforwardly identified in the Hilbert space of a two-physical-qubit system. Indeed, as the two-qubit states $\{|0_{DFS}\rangle \equiv |01\rangle, |1_{DFS}\rangle \equiv |10\rangle\}$ are affected in the same way by phase errors

$$|0_{DFS}\rangle \equiv |01\rangle \overset{t}{\rightarrow} \exp\left(-i\int_0^t [\epsilon_0(\tau) + \epsilon_1(\tau)]d\tau\right)|01\rangle,$$

$$|1_{DFS}\rangle \equiv |10\rangle \overset{t}{\rightarrow} \exp\left(-i\int_0^t [\epsilon_0(\tau) + \epsilon_1(\tau)]d\tau\right)|10\rangle,$$

the subspace they span is clearly left invariant by the errors. This shows that a qubit of information can be safely stored in the state of a two-physical-qubit system.

From a practical point of view, in order to protect the information contained in a physical qubit initially in the state $|\psi\rangle = c_0|0\rangle + c_1|1\rangle$, one simply adds a second auxiliary qubit, initially prepared in the state $|1\rangle$ and performs a CNOT gate, which achieves the DFS encoding

$$|\psi\rangle|1\rangle = c_0|01\rangle + c_1|11\rangle \overset{\text{CNOT}}{\rightarrow} c_0|01\rangle + c_1|10\rangle = |\psi_{DFS}\rangle.$$

Decoding is straightforwardly performed through applying the CNOT gate again. Moreover, a protected N-logical-qubit memory can be constructed just by associating N protected cells, which requires $2N$ physical qubits.

To process the information safely stored in the DFS we now need to design a new set of universal gates, comprising the single-logical-qubit Hadamard and $\pi/8$ gates, as well as the two-logical-qubit CNOT gate. This point is actually not obvious. Indeed, the gate implementations proposed in [10] cannot be used any longer as they would make the system leave the DFS, resulting in erroneous calculations. We thus have to resort to new physical primitives. In the following we review two secure processes that constantly remain in the DFS. We then show how to combine them to implement universal protected computation.

B. Physical primitives for universal protected computation

The first primitive consists of a phase gate, obtained through applying a laser to the first atom of the logical qubit. The Rabi frequency is denoted Ω_d and the laser frequency ω_d is detuned by the quantity Δ_d from the frequency ω of the transition $|1\rangle \rightarrow |e\rangle$ where $|e\rangle$ denotes an excited state (Δ_d

$\equiv \omega_d - \omega$; see Fig. 2). After a time $t_d = n2\pi/\Omega_{R,d}$, where $\Omega_{R,d} = \sqrt{|\Omega_d|^2 + \Delta_d^2}$ and n is a positive integer, the state $|10\rangle$ picks up the phase factor $e^{i\varphi}$, where $\varphi = n\pi(1 + \Delta_d/\Omega_{R,d})$, while the state $|01\rangle$ is left unchanged. In the DFS basis, this transformation is represented by the matrix

$$P(\varphi) = \begin{bmatrix} 1 & 0 \\ 0 & e^{i\varphi} \end{bmatrix}.$$

Given an arbitrary phase φ_0 one can choose the different physical parameters such that $\varphi = \varphi_0$ and $|\Delta_d| \gg |\Omega_d|$, which ensures that the excited state $|e\rangle$ remains essentially unpopulated during the process.

The second primitive is implemented by applying two laser fields $\vec{E}_i(t) = \frac{1}{2}(\vec{E}_{0,i} e^{-i(\omega_i t - \varphi_i)} + \text{c.c.})$, $i = 1, 2$, to a pair of atoms. The frequencies ω_i are assumed slightly detuned from the transitions $|i\rangle \to |r\rangle$, $i = 0, 1$, respectively, where $|r\rangle$ is a Rydberg state of the atom. The detunings are denoted [see Fig. 3(a)]

$$\Delta = \omega_0 - \omega_{0r} \quad \text{and} \quad \Delta' = \omega_0 - \omega_1 - \omega_{01},$$

where ω_{ir} is the frequency of the transition $|i\rangle \to |r\rangle$. Let us emphasize that the two atoms involved in the transformation are not bound to belong to the same logical qubit, i.e., they do not have to be in a superposition of the states $|01\rangle$ and $|10\rangle$.

As is well known [21], Rydberg atoms exhibit huge dipole moments which lead to large dipole-dipole interactions responsible for dipole blockade [9]. We shall assume that the dipole-dipole interaction is only significant when both atoms are in their Rydberg states $|r\rangle$. In other words, we shall assume $\hat{V}_{dd} = \hbar\Delta_{rr}|rr\rangle\langle rr|$. When the fields are applied to a pair of atoms, transitions may occur between the different resonant physical qubit product states, in agreement with energy conservation. We observe that the states $|00\rangle$ and $|11\rangle$ couple to themselves to second order, and, as the doubly excited Rydberg state $|rr\rangle$ is shifted far off resonance due to the dipole-dipole interaction, the only two paths actually coupling $|01\rangle$ and $|10\rangle$ are the two fourth-order M systems drawn on Fig. 3(b).

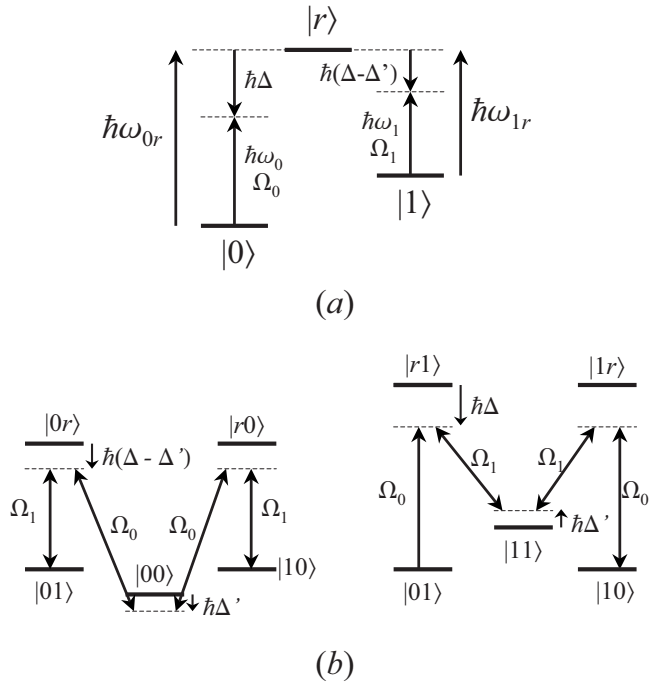

FIG. 3. (a) Level scheme and laser couplings for one atom. (b) The two M-shaped paths coupling $|01\rangle$ and $|10\rangle$.

Assuming $|\Omega_0|, |\Omega_1| \ll |\Delta|, |\Delta'|, |\Delta' - \Delta|, |\Delta_{rr}|$, one can extract the effective dynamics of the subspace $\{|00\rangle, |01\rangle, |10\rangle, |11\rangle\}$ through a perturbative approach [22] which yields the evolution operator, expressed in the interaction picture,

$$U_{eff}(t, \Omega_0, \Omega_1, \Delta, \Delta', \Delta_{rr}) = e^{-i(\Delta_0 - \Delta')t} \times \begin{bmatrix} e^{-i(\Delta_{00} - \Delta_0)t} & 0 & 0 & 0 \\ 0 & \cos\left(\frac{\Omega_R t}{2}\right) & i\sin\left(\frac{\Omega_R t}{2}\right) & 0 \\ 0 & i\sin\left(\frac{\Omega_R t}{2}\right) & \cos\left(\frac{\Omega_R t}{2}\right) & 0 \\ 0 & 0 & 0 & e^{-i(\Delta_{11} - \Delta_0)t} \end{bmatrix}$$

where

$$\Omega_R = \frac{|\Omega_0 \Omega_1|^2}{8} \frac{\Delta_{rr}(\Delta' - 2\Delta)}{(\Delta_{rr} + \Delta' - 2\Delta)\Delta^2(\Delta' - \Delta)^2}, \tag{1}$$

$$\Delta_0 = \frac{|\Omega_0|^2}{4\Delta} + \frac{|\Omega_1|^2}{4(\Delta - \Delta')} - \frac{1}{16}\left(\frac{|\Omega_0|^4}{\Delta^3} + \frac{|\Omega_1|^4}{(\Delta - \Delta')^3} + \frac{|\Omega_0 \Omega_1|^2 (2\Delta_{rr} + \Delta' - 2\Delta)(2\Delta - \Delta')}{(\Delta_{rr} + \Delta' - 2\Delta)\Delta^2(\Delta' - \Delta)^2}\right), \tag{2}$$

$$\Delta_{00} = \frac{|\Omega_0|^2}{2\Delta}\left[1 + \frac{1}{2\Delta}\left(\frac{|\Omega_1|^2}{2\Delta'} - \frac{|\Omega_0|^2(\Delta_{rr} - \Delta)}{\Delta(\Delta_{rr} - 2\Delta)}\right)\right], \tag{3}$$

$$\Delta_{11} = \frac{|\Omega_1|^2}{2(\Delta - \Delta')}\left[1 + \frac{1}{2(\Delta' - \Delta)}\left(\frac{|\Omega_0|^2}{2\Delta'} + \frac{|\Omega_1|^2(\Delta_{rr} + \Delta' - \Delta)}{(\Delta - \Delta')(\Delta_{rr} + 2\Delta' - 2\Delta)}\right)\right]. \quad (4)$$

It is important to note that if the two atoms involved are initially prepared in a DFS state, i.e., in a superposition of $|01\rangle$ and $|10\rangle$, the transformation U_{eff} leaves them in the DFS and the associated gate

$$R(\theta) \propto \begin{bmatrix} \cos(\theta) & i\sin(\theta) \\ i\sin(\theta) & \cos(\theta) \end{bmatrix} \quad \text{with } \theta \equiv \frac{\Omega_R t}{2},$$

is thus safe. But it is also interesting to note that if the two atoms considered are not in a DFS state, as for example in the state $|00\rangle$, they pick up a phase factor, which can be controlled via the Rabi frequencies and detunings. This observation will be used in the following to implement a two-logical-qubit phase gate.

To conclude, let us emphasize that the transformations we have just considered are not completely error-free. They are safe in the sense that they do not make the system leave the DFS, the information thus being constantly protected from the effect of the errors. But the errors will of course affect the primitives P and U_{eff} (and thus the gates we shall build by combining them) through the detunings Δ, Δ', Δ_{rr} which will take slightly different values from the ideally expected ones. However, the detunings being large, the effect of reasonably small errors on the system will be quite unnoticeable. The limitation of the fidelity for the quantum gates will be numerically analyzed in the following section.

C. Construction of universal safe quantum gates

Let us now see how the previous primitives can be used to implement universal safe computation. The single-logical-qubit $\pi/8(T)$ and Hadamard (H) gates are straightforwardly obtained according to

$$T_{DFS} \equiv \begin{bmatrix} 1 & 0 \\ 0 & e^{i\pi/4} \end{bmatrix} \propto P\left(\frac{\pi}{4}\right),$$

$$H_{DFS} \equiv \frac{1}{\sqrt{2}}\begin{bmatrix} 1 & 1 \\ 1 & -1 \end{bmatrix} \propto P\left(\frac{3\pi}{2}\right)R\left(\frac{\pi}{4}\right)P\left(\frac{3\pi}{2}\right).$$

We now consider two logical qubits, consisting of the physical qubits (1, 2) and (3, 4), respectively. The information is naturally encoded on the decoherence free (code) subspace $\mathcal{C}$, spanned by

$$|00\rangle_{DFS} \equiv |0101\rangle,$$

$$|01\rangle_{DFS} \equiv |0110\rangle,$$

$$|10\rangle_{DFS} \equiv |1001\rangle,$$

$$|11\rangle_{DFS} \equiv |1010\rangle.$$

This four-dimensional DFS can be extended into a six-dimensional DFS $\mathcal{D}$ through adding the two vectors $|\alpha\rangle_{DFS} \equiv |0011\rangle$ and $|\beta\rangle_{DFS} \equiv |1100\rangle$ to $\mathcal{C}$: as the vectors $|\alpha\rangle_{DFS}$, $|\beta\rangle_{DFS}$, $|00\rangle_{DFS}$, $|01\rangle_{DFS}$, $|10\rangle_{DFS}$, and $|11\rangle_{DFS}$ contain the same number of 0's (and 1's), they are affected in the same way by the phase errors. It is also important to note that, whereas in the states $|00\rangle_{DFS}$, $|01\rangle_{DFS}$, $|10\rangle_{DFS}$, and $|11\rangle_{DFS}$ the logical qubits (1, 2) and (3, 4) are individually protected, in the states $|\alpha\rangle_{DFS}$ and $|\beta\rangle_{DFS}$ only the pair of logical qubits is protected. Let us now see how to perform a two-qubit gate on the information initially stored in $\mathcal{C}$. One might think that in order to implement a logical two-qubit gate a four-atom process must be involved. It turns out, however, that a two-atom operation is sufficient to implement a controlled phase gate between two logical qubits. Thus consider the transformation $U_{eff}^{(1,3)}(\tau, \Omega_0, \Omega_1, \Delta, \Delta', \Delta_{rr})$ involving atoms 1 and 3 from different DFS pairs, cf. Fig. 4. This operation transforms the states $\{|00\rangle_{DFS}, |01\rangle_{DFS}, |10\rangle_{DFS}, |11\rangle_{DFS}\}$ according to

$$|00\rangle_{DFS} \to e^{-i(\Delta_{00} - \Delta')t}|00\rangle_{DFS},$$

$$|01\rangle_{DFS} \to e^{-i(\Delta_0 - \Delta')t}\left[\cos\left(\frac{\Omega_R t}{2}\right)|01\rangle_{DFS} + i\sin\left(\frac{\Omega_R t}{2}\right)|\beta\rangle_{DFS}\right],$$

$$|10\rangle_{DFS} \to e^{-i(\Delta_0 - \Delta')t}\left[\cos\left(\frac{\Omega_R t}{2}\right)|10\rangle_{DFS} + i\sin\left(\frac{\Omega_R t}{2}\right)|\alpha\rangle_{DFS}\right],$$

$$|11\rangle_{DFS} \to e^{-i(\Delta_{11} - \Delta')t}|11\rangle_{DFS}.$$

In other words, even though the system leaves the code space $\mathcal{C}$, it constantly remains in the extended DFS $\mathcal{D}$ which ensures that the information is protected from the action of phase errors. Moreover, if we adjust the different parameters in such a way that

$$t = \tau = \frac{4\pi}{\Omega_R}, \quad \frac{\Delta_{00} - \Delta_0}{\Omega_R} = \frac{k}{2}, \quad \frac{\Delta_{11} - \Delta_0}{\Omega_R} = \frac{1}{4} + \frac{l}{2}, \quad (5)$$

where k, l are integers, $U_{eff}^{(1,3)}$ transforms the vectors of $\mathcal{C}$ according to

$$|00\rangle_{DFS} \to e^{-i(\Delta_0 - \Delta')t}|00\rangle_{DFS},$$

$$|01\rangle_{DFS} \to e^{-i(\Delta_0 - \Delta')t}|01\rangle_{DFS},$$

$$|10\rangle_{DFS} \to e^{-i(\Delta_0 - \Delta')t}|10\rangle_{DFS},$$

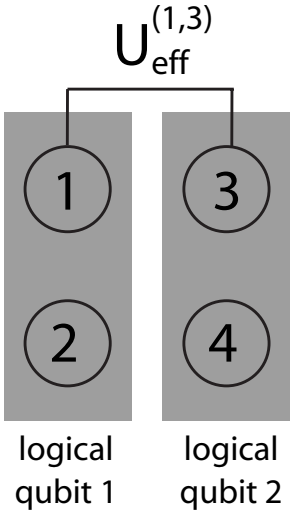

FIG. 4. The U_{eff} gate acting on atoms 1 and 3.

$$|11\rangle_{DFS} \rightarrow -e^{-i(\Delta_0-\Delta')t}|11\rangle_{DFS},$$

which corresponds to a protected conditional phase gate $U_{phase,DFS}$ on the code subspace $\mathcal{C}$. It is now straightforward to implement the protected CNOT gate

$$\text{CNOT}_{DFS} = (I \otimes H_{DFS}) \times U_{phase,DFS} \times (I \otimes H_{DFS})$$

(cf. Fig. 5), which completes our set of protected universal quantum gates.

IV. NUMERICAL SIMULATIONS

As already pointed out, the gates we have just implemented are not error-free, as their fidelities are limited by the errors that modify the detunings involved. Spontaneous emission from the excited states $|e\rangle$ and $|r\rangle$ also restricts the performances of our gates, and has to be taken into account. In this section, we numerically estimate the influence on the fidelity of random phase errors and spontaneous emission and compare the protected gates to a set of unprotected gates. Finally, we discuss the practical interest and feasibility of our proposal.

A. Performances of the protected gates

In this section, we first describe how phase errors and spontaneous emission are modeled in our system. Then we introduce the fidelity measure we shall use throughout this section. Finally we explain how simulations are performed, and discuss our results in detail.

Here we assume phase errors on $|1\rangle$, $|e\rangle$, and $|r\rangle$ and model their effect by the single-atom Hamiltonian

$$\hat{E}(t) = \hbar[\epsilon_1(t)|1\rangle\langle 1| + \epsilon_e(t)|e\rangle\langle e| + \epsilon_r(t)|r\rangle\langle r|].$$

Moreover, we suppose that phase errors can be described by an Ornstein-Uhlenbeck process for which [23]

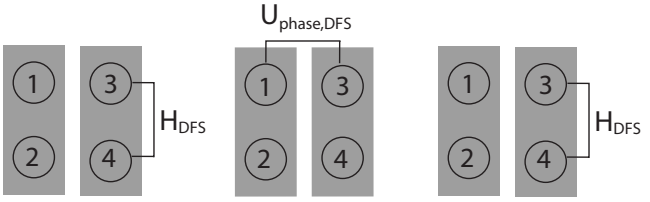

FIG. 5. The CNOT_{DFS} gate.

$$\epsilon(t+dt) = \epsilon(t) - \frac{1}{\tau}\epsilon(t)dt + \sqrt{c}G(t)\sqrt{dt}$$

where τ is the relaxation time, c is the diffusion constant, and $G(t)$ is the unit Gaussian variable. The Ornstein-Uhlenbeck process is characterized by the correlation function

$$\langle \epsilon(t)\epsilon(t')\rangle = \frac{\tau c}{2}e^{-|t-t'|/\tau}$$

in steady state. We assume that the errors for the various levels are correlated, which seems reasonable for background magnetic field perturbations. Thus $\epsilon_1(t)$ is generated using the approach described above while $\epsilon_e(t)$ and $\epsilon_r(t)$ are found from $\epsilon_e(t)=\alpha_e\epsilon_1(t)$ and $\epsilon_r(t)=\alpha_r\epsilon_1(t)$.

Spontaneous emission from the excited state (used for the implementation of the P gate) and the Rydberg state can be taken into account by adding the term $-i\hbar\left[\frac{\gamma_e}{2}|e\rangle\langle e| + \frac{\gamma_r}{2}|r\rangle \times \langle r|\right]$ to the single-atom Hamiltonian. For the numerical implementation we have considered $|e\rangle=|r\rangle$. The radiative linewidth of the Rydberg state, $\gamma_r/2\pi$, is estimated to be smaller than 10 kHz for $n>65$ [10].

An appropriate fidelity measure for the performance of the gates in the presence of stochastic errors is calculated in the following way. For an $N\times N$ density matrix, ρ, the time evolution is given by $\rho \overset{U}{\rightarrow} U\rho U^\dagger$. Representing the matrix ρ as a vector $\vec{\rho}$ this can be rewritten such that $\vec{\rho} \overset{U}{\rightarrow} M\vec{\rho}$ with M being an $N^2\times N^2$ matrix. To each instance of $\epsilon_1(t)$ [and correspondingly $\epsilon_e(t)$ and $\epsilon_r(t)$] corresponds a certain M. In order to obtain an average over the various phase error configurations, we can now simply average over the corresponding M's and subsequently calculate the fidelity from

$$F(|\psi\rangle) = \vec{\rho}^\dagger_{ideal} M_{av} \vec{\rho}$$

where $\rho_{ideal}=U_{ideal}\rho U^\dagger_{ideal}$, M_{av} denotes the average over M and $\rho=|\psi\rangle\langle\psi|$. In practice, we evaluate F for a large number of pure states $|\psi\rangle$, and in the figures we present the minimum value of F over these input states.

As shown in the previous section, the different universal gates can be obtained by combination of the two primitives $P(\varphi)$ and $U_{\text{eff}}(t,\Omega_0,\Omega_1,\Delta,\Delta',\Delta_{rr})$: it is thus necessary to perform these primitives with high precision. The expression obtained for $P(\varphi)$ is exact: it implies that, in the absence of errors and spontaneous emission, if we tune $\{n,\Omega_d,\Delta_d\}$ such that $\varphi=n\pi(1+\Delta_d/\sqrt{|\Omega_d|^2+|\Delta_d|^2})$ is the desired phase factor, we shall exactly get the expected phase gate $P(\varphi)$. On the

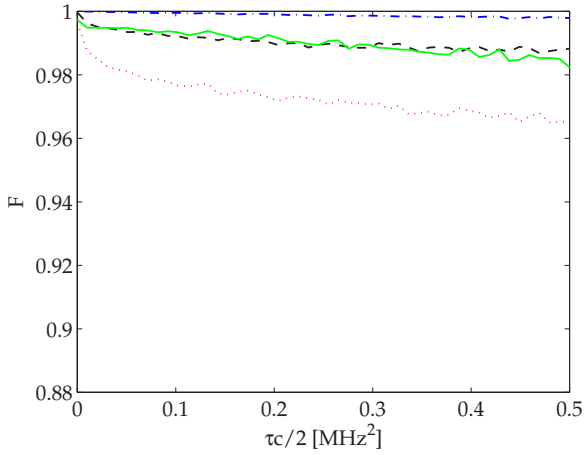

FIG. 6. (Color online) Performance of the universal set of gates without spontaneous emission. Dash-dotted, T_{DFS}; dashed, H_{DFS}; solid line, $U_{phase,DFS}$; dotted, CNOT_{DFS}. Parameters for the gates are as follows, P gate: $\Omega_d/2\pi=5$ MHz, $\Delta_d/2\pi\approx-49.81$ MHz, $t(\pi/4)\approx1.00$ μs. $R(\pi/4)$ gate: $\Omega_0/2\pi\approx3.91$ MHz, $\Omega_1/2\pi\approx1.97$ MHz, $\Delta/2\pi\approx60.34$ MHz, $\Delta'/2\pi\approx30.70$ MHz, $\Delta_{rr}/2\pi=100$ MHz, $t\approx120.20$ μs. $U_{phase,DFS}$ gate: $\Omega_0/2\pi\approx3.93$ MHz, $\Omega_1/2\pi\approx1.96$ MHz, $\Delta/2\pi\approx60.48$ MHz, $\Delta'/2\pi\approx30.05$ MHz, $\Delta_{rr}/2\pi=100$ MHz, $t\approx938.62$ μs. For the generation of the phase errors the parameters are $\tau=1$ μs, $\alpha_e=\alpha_r=1.5$.

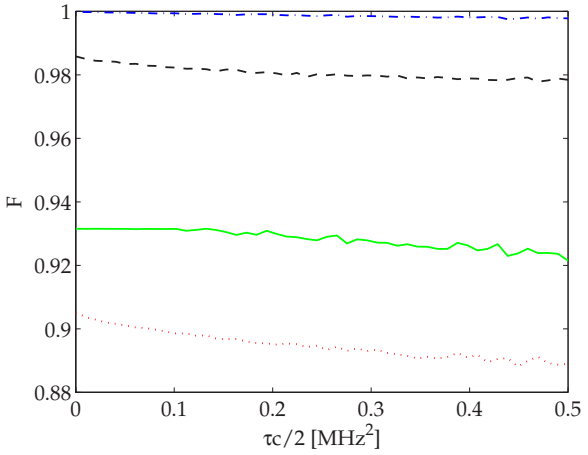

FIG. 7. (Color online) Performance of the gates including spontaneous emission with $\gamma_r/2\pi=5$ kHz. Parameters and notations are the same as for Fig. 6.

contrary, the expression we obtained for U_{eff} is only perturbative. It means that if we choose the physical parameters $\{t,\Omega_0,\Omega_1,\Delta,\Delta',\Delta_{rr}\}$ so that the effective parameters Eqs. (1)–(4) take the desired values [to implement a conditional phase gate or an $R(\theta)$ gate], the exponential of the full Hamiltonian will be slightly different from the desired gate, even in the ideal case. Before dealing with errors and spontaneous emission, we refine the parameters by a numerical search in the neighborhood of our first guess provided by the analytical perturbative approach. Once we have a faithful gate in the ideal case, we keep the same set of parameters and include the new terms discussed above in the Hamiltonian in order to run our simulations.

Figures 6 and 7 show the performances of the different gates when spontaneous emission is not (is) included, respectively. The fidelity is plotted as a function of $\tau c/2$, which corresponds to the variance of the detuning due to perturbations. As is evident in Fig. 7 spontaneous emission severely limits the fidelity.

Note that in [10] the transitions to the Rydberg states are implemented by going off-resonantly via $|5P_{1/2}\rangle$. This worsens the problem of spontaneous emission, as the R and $U_{phase,DFS}$ gates are thus quite slow and the radiative linewidth for the $|5P_{1/2}\rangle$ state is quite large ($\gamma_{5P_{1/2}}/2\pi=5.7$ MHz). It is thus necessary to be strongly detuned from the level $|5P_{1/2}\rangle$, but as this reduces the coupling to the Rydberg levels, the intensity of the Raman beams should at the same time be increased.

A further source of decoherence for the experimental setup proposed in [10] is the motion of atoms in the traps: as the interatomic distance, R, varies so does the dipole-dipole interaction, which scales as $1/R^3$. Based on estimates provided in [10] a variation of 20% for the value of Δ_{rr} is expected. We performed a numerical simulation assuming that Δ_{rr} is harmonically varying which demonstrated a dramatic reduction of the fidelity for realistic parameters. Atomic motion in the traps thus poses a serious limitation for the gates. To improve the performances of the gates the atoms might be cooled further or the distance between the traps could be increased, which would, however, reduce Δ_{rr}.

B. Comparison with unprotected gates

In order to assess the performance of the universal set of DFS gates suggested in this paper, we compare them to a universal set of unprotected gates.

If we remove the restriction that the system should remain in the DFS at all times, a controlled-phase gate between two atoms can be carried out as suggested in [9] in the regime of a large interaction strength. Combining this gate with two single-atom Hadamard gates, which are obtained through single-atom rotations between states $|0\rangle$ and $|1\rangle$ via an excited state, results in a two-atom CNOT gate. A universal set of gates is then given by

$$H_{DFS}=\mathrm{CNOT}_{1,2}\times(H\otimes I)\times\mathrm{CNOT}_{1,2}$$

$$\mathrm{CNOT}_{DFS}=\mathrm{CNOT}_{1,3}\times\mathrm{CNOT}_{1,4}$$

where $\mathrm{CNOT}_{i,j}$ is a CNOT gate with atom i being the control qubit and atom j being the target qubit. The T_{DFS} gate is simply implemented in the same way as for the protected gates.

In Fig. 8 we plot the performance of the unprotected Hadamard and CNOT gates. As expected, these gates are much more sensitive to phase errors than the protected gates. Spontaneous emission from the Rydberg states also severely limits the fidelity for the unprotected gates, as the controlled-phase gate involves resonant transitions to the Rydberg levels.

The durations of the gates are, however, smaller than for the protected gates. Thus, with the parameters for Fig. 8 the durations of the gates are $t(H_{DFS})=15.5$ μs and $t(\mathrm{CNOT}_{DFS})=14$ μs.

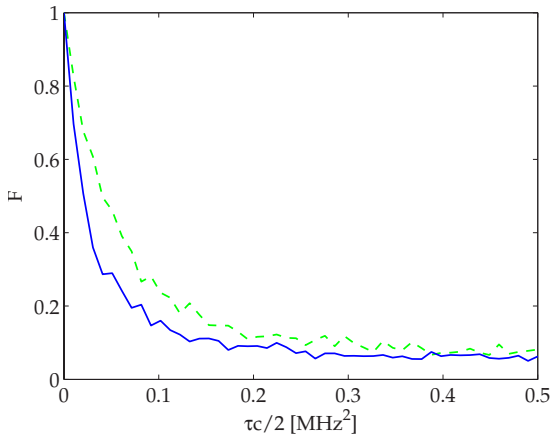

FIG. 8. (Color online) Performance for the unprotected gates. Dashed, H_{DFS}; solid line, CNOT_{DFS}. Parameters: $\Omega/2\pi=0.5$ MHz, $\Delta_{rr}/2\pi=100$ MHz, $\tau=1$ μs, $\alpha_e=\alpha_r=1.5$.

Another advantage of the unprotected gates as opposed to the protected ones we have suggested is that they are less sensitive to variations in Δ_{rr}, and thus to atomic motion.

V. CONCLUSION

In this paper we have identified a set of logical qubit basis states for a neutral-atom decoherence-free subspace and a corresponding set of protected universal gates. Numerical simulations demonstrate that the proposed set of gates is much more robust against phase errors than a set of unprotected gates. They are, however, also much more affected by the motion of the atoms in the traps. Therefore, one has to consider what the worst source of decoherence is for a given physical situation and subsequently choose which set of gates to use. Even if the set of protected gates is assessed to be unfavorable, one should still consider using the logical qubit bases states for computations, as information is then protected during storage of the qubits.

The work presented in this paper naturally leads to further developments. First, we would like to study resource optimized DFS encoding. Here, in order to build a reliable $N=2$–qubit register we have merely associated two two-physical-qubit protected cells, but it is clear that for an N-qubit quantum memory ($N\geqslant 3$) the number of physical qubits required by this straightforward scheme, i.e., $2N$ physical qubits, is much larger than actually needed. This construction of a DFS will induce other problems, as regards practical encoding and processing of the information stored in the DFS, the resolution of which will probably require the use of quantum control techniques, such as nonholonomic control [24]. Moreover, we also plan to extend our results to more general error models such as, for instance, position-dependent errors.

ACKNOWLEDGMENTS

This work was supported by ARO-DTO Grant No. 47949PHQC. S.C. and M.S. were also supported by NSF Grant No. PHY-0205236 and K.M. was supported by the European Union integrated project SCALA.

[1] M. A. Nielsen and I. L. Chuang, *Quantum Computation and Quantum Information* (Cambridge University Press, Cambridge, U.K., 2000).
[2] D. Deutsch, Proc. R. Soc. London, Ser. A **400**, 97 (1985).
[3] R. P. Feynman, Int. J. Theor. Phys. **21**, 467 (1982).
[4] P. W. Shor, SIAM J. Comput. **26**, 1484 (1997).
[5] N. Gershenfeld and I. L. Chuang, Science **275**, 350 (1997).
[6] P. Domokos, J. M. Raimond, M. Brune, and S. Haroche, Phys. Rev. A **52**, 3554 (1995).
[7] J. I. Cirac and P. Zoller, Phys. Rev. Lett. **74**, 4091 (1995).
[8] D. P. DiVincenzo, Fortschr. Phys. **48**, 771 (2000).
[9] D. Jaksch, J. I. Cirac, P. Zoller, S. L. Rolston, R. Côté, and M. D. Lukin, Phys. Rev. Lett. **85**, 2208 (2000).
[10] M. Saffman and T. G. Walker, Phys. Rev. A **72**, 022347 (2005).
[11] D. Gottesman, Phys. Rev. A **54**, 1862 (1996).
[12] G. M. Palma, K.-A. Suominen, and A. K. Ekert, Proc. R. Soc. London, Ser. A **452**, 567 (1996); P. Zanardi and M. Rasetti, Phys. Rev. Lett. **79**, 3306 (1997); D. A. Lidar and K. B. Whaley, in *Irreversible Quantum Dynamics*, edited by F. Benatti and R. Floreanini, Springer Lecture Notes in Physics Vol. 622 (Springer, Berlin, 2003), pp. 83–120.
[13] L. M. Duan and G. C. Guo, Phys. Rev. Lett. **79**, 1953 (1997); D. A. Lidar, I. L. Chuang, and K. B. Whaley, *ibid.* **81**, 2594 (1998).
[14] D. A. Lidar, D. Bacon, J. Kempe, and K. B. Whaley, Phys. Rev. A **63**, 022306 (2001).
[15] A. Shabani and D. A. Lidar, Phys. Rev. A **72**, 042303 (2005).
[16] P. G. Kwiat, A. J. Berglund, J. B. Altepeter, and A. G. White, Science **290**, 498 (2000).
[17] D. Kielpinski, V. Meyer, M. A. Rowe, C. A. Sackett, W. M. Itano, C. Monroe, and D. J. Wineland, Science **291**, 1013 (2001).
[18] P. Xue and Y.-F. Xiao, Phys. Rev. Lett. **97**, 140501 (2006).
[19] J. E. Ollerenshaw, D. A. Lidar, and L. E. Kay, Phys. Rev. Lett. **91**, 217904 (2003).
[20] D. Bacon, J. Kempe, D. A. Lidar, and K. B. Whaley, Phys. Rev. Lett. **85**, 1758 (2000); J. Kempe, D. Bacon, D. A. Lidar, and K. B. Whaley, Phys. Rev. A **63**, 042307 (2001); D. A. Lidar, D. Bacon, J. Kempe, and K. B. Whaley, *ibid.* **63**, 022307 (2001); L. Viola and E. Knill, Phys. Rev. Lett. **90**, 037901 (2003).
[21] T. F. Gallagher, *Rydberg Atoms* (Cambridge University Press, Cambridge, U.K., 1994).
[22] F. H. M. Faisal, *Theory of Multiphoton Processes* (Plenum Press, New York, 1987).
[23] D. T. Gillespie, Am. J. Phys. **64**, 225 (1996).
[24] G. Harel and V. M. Akulin, Phys. Rev. Lett. **82**, 1 (1999); E. Brion, D. Comparat, and G. Harel, Eur. Phys. J. D **38**, 381 (2006).